J. Appl. Environ. Biol. Sci., 5(12)125-136, 2015
© 2015, TextRoad Publication

ISSN: 2090-4274
Journal of Applied Environmental and Biological Sciences
www.textroad.com

Viscoelastic Immiscible Double Layer Fluid Flow over Outside Surface of a Vertical Cylinder

Rehan Ali Shah, Muhammad Waqar Khan

Department of Basic Sciences & Islamiat, University of Engineering & Technology Peshawar, KPK, Pakistan

Received: August 12, 2015
Accepted: October 30, 2015

ABSTRACT

The aim of this paper is to describe the flow of a double layer viscoelastic fluid flowing down a vertical cylinder. Constitutive equations for Phan-Thein and Tanner (PTT) fluid are used in the mathematical modeling. The exact solution for velocity field, flow rate and shear stresses are derived for both the layers. For better understanding analytical results for flow rate, shear stresses and for velocity fields are obtained. Effects of physical quantities like viscosity, density, elongation and relaxation parameter are investigated for velocity field, flow rate and for shear stresses.

KEYWORDS: Double Layer, Immiscible Flow, PTT Fluid, Gravity Flow.

1. INTRODUCTION

In recent past years, the study of non-Newtonian Viscoelastic fluids in Engineering Sciences and especially on industry side play an important role in manufacturing process, polymer solution, etc. On the other side, the applications of non-Newtonian Viscoelastic fluids are of paper finishing, food packing, coating etc. Further, the use of double layer viscoelastic fluids is of particular interest like double layer coating, double layer paints in various chemical processing. Relevant and attractive work related to single layer with same geometry may be found in the following published articles. Taza Gul et al. [1, 2] studied thin film flow of a single layer third order electrically conducted fluid with slip and no slip conditions. They derived velocity field and temperature distribution by Adomian Decomposition Method. Hayat et al. [3] discussed the analytic solution of thin film flow of a fourth grade fluid down a vertical cylinder. They obtained the velocity field using Homotopy Analysis Method. Sajid et al. [4] studied Wire coating analysis using MHD Oldroyd8-constant fluid. Smith et al. [5] investigate the unsteady free-surface flow of a Newtonian fluid issuing vertically upwards from a tube in the base of a vertical cylindrical cavity. The velocity of two immiscible and incompressible fluids between two parallel plates is discussed by Bird et al. [6] It was shown there that when the heights of two fluids are equal, then the velocity of the less viscous fluid becomes maximum as compare to the more viscous fluid. In the meantime, Kapur et al. [7] discussed the maximum velocity of both fluids at differentpoints and their interface. Later on Kapur et al. [8] discuss the flow of immiscible fluids between two plates of different heights. They have shown that whatever the number of fluids and whatever their heights are, a unique velocity maximum always exists. The flow of two immiscible fluids with uniform suction at the stationary plate was discussed by Sacheti [9]. He notified that the suction is to supply an adverse pressure gradient causing back flow near the stationary plate. Anne Juel et al. [10] studied the experimental observations of two liquid layers in reasonable agreement with linear stability analyses. The comparisons between classical non Newtonian EHL and non-Newtonian TFEHL are discussed by Hsiao-Ming Chu et al. [11] Recently Kim et al. [12] studied double layer coating liquid flows. Their approximations are based on Laminar flow and Power Law Model of non-Newtonian fluids. They discussed the coating liquid flow of immiscible resin in model of capillary annuls, where the surface of glass fiber moves at high fiber drawing speed. Dandapat et al. [13] discussed unsteady two-layer liquid film of uniform thickness on a horizontal rotating disk for small values of Reynolds number. Zeeshan et al. [14] studied the behavior of an incompressible viscoelastic PTT fluid in the double layer coating liquid flow inside a secondary coating die of the optical fiber coating applicator. Due to applications of double layer coating analysis will be made for double layer viscoelastic fluid on vertical cylinder. According to best of our knowledge there is no literature available of the stated problem.

2. Basic equation

The basic equations governing the flow of an incompressible fluid are:

$$\nabla . \bar{u}_i = 0, \tag{1}$$

$$\rho_i \frac{D\bar{u}_i}{Dt} = \bar{\nabla} . \bar{T}_i + \rho_i \bar{g}, \qquad i = 1, 2 . \tag{2}$$

The subscripts $i = 1, 2$ represent layer 1 and layer 2,

***Corresponding author:** Rehan Ali Shah, Department of Basic Sciences & Islamiat UET, Peshawar, KPK, Pakistan.
Email ID: mmrehan79@yahoo.com

where $\bar{u}_i$ is the fluid velocity, ρ_i is constant density,$\bar{T}_i$ is stress tensor, $\bar{g}$ denotes gravity and $\frac{D}{Dt}$ is the material derivative. The stress tensor $\bar{T}_i$ is defined as

$$\bar{T}_i = -p_i\bar{I} + \bar{\tau}_i \tag{3}$$

In which I is Identity tensor, $\bar{\tau}_i$ is shear stress and p_i is the pressure.

Cylindrical component of continuity equation can be written as

$$\frac{1}{r}\frac{\partial r u_{ir}}{\partial r} + \frac{1}{r}\frac{\partial u_{i\theta}}{\partial \theta} + \frac{\partial u_{iz}}{\partial z} = 0 \tag{4}$$

Equations of motion in cylindrical co-ordinate system are:

r-component of momentum equation

$$\rho_i\left(\frac{\partial u_{ir}}{\partial t} + u_{ir}\frac{\partial u_{ir}}{\partial r} + \frac{u_{ir}}{r}\left(\frac{\partial u_{ir}}{\partial \theta} - \frac{u_{i\theta}}{r}\right) + u_{iz}\frac{\partial u_{ir}}{\partial z}\right) = -\frac{\partial p_i}{\partial r} + \left(\frac{1}{r}\frac{\partial (r\tau_{irr})}{\partial r} + \frac{1}{r}\frac{\partial \tau_{ir\theta}}{\partial \theta} - \frac{\tau_{i\theta\theta}}{r} + \frac{\partial \tau_{irz}}{\partial z}\right) + \rho_i g_r \tag{5}$$

θ-component of momentum equation

$$\left(\frac{\partial u_{i\theta}}{\partial t} + u_{ir}\frac{\partial u_{i\theta}}{\partial r} + \frac{u_{i\theta}}{r}\left(\frac{\partial u_{i\theta}}{\partial \theta} + \frac{u_{ir}}{r}\right) + u_{iz}\frac{\partial u_{i\theta}}{\partial z}\right) = -\frac{1}{r}\frac{\partial p_i}{\partial \theta} + \left(\frac{1}{r^2}\frac{\partial (r^2\tau_{ir\theta})}{\partial r} + \frac{1}{r}\frac{\partial \tau_{i\theta\theta}}{\partial \theta} + \frac{\partial \tau_{i\theta z}}{\partial z}\right) + \rho_i g_\theta \tag{6}$$

z-component of momentum equation

$$\rho_i\left(\frac{\partial u_{iz}}{\partial t} + u_{ir}\frac{\partial u_{iz}}{\partial r} + \frac{u_{i\theta}}{r}\frac{\partial u_{iz}}{\partial \theta} + u_{iz}\frac{\partial u_{iz}}{\partial z}\right) = -\frac{\partial p_i}{\partial z} + \left(\frac{1}{r}\frac{\partial (r\tau_{irz})}{\partial r} + \frac{1}{r}\frac{\partial \tau_{i\theta z}}{\partial \theta} + \frac{\partial \tau_{izz}}{\partial z}\right) + \rho_i g_z \tag{7}$$

The general form of the constitutive equation for Phan-Thien Tanner (PTT) fluid is given by

$$f_i(tra\bar{\tau}_i)\bar{\tau}_i + \lambda_i\bar{\tau}_i^{\Delta} = 2\eta_i\bar{D}_i \qquad i = 1, 2, \tag{8}$$

where $\bar{\tau}_i$ and $\bar{D}_i$ are the extra-stress and deformation-rate tensors, λ_i is the relaxation time $\eta_i$is constant viscosity coefficient and $\bar{\tau}_i^{\Delta}$ denotes upper-convected derivative, and

$$\bar{D}_i = \bar{L}_i^T + \bar{L}_i\,, \tag{9}$$

and

$$\bar{\tau}_i^{\Delta} = \frac{D\bar{\tau}_i}{Dt} - [\bar{\tau}_i(\nabla\bar{u}_i) + (\nabla\bar{u}_i)^T\bar{\tau}_i] \qquad i = 1, 2. \tag{10}$$

The linearized form of PTT model is

$$f_i\,(tra\bar{\tau}_i) = 1 + \frac{\epsilon_i\lambda_i}{\eta_i}(tra\bar{\tau}_i) \qquad i = 1, 2. \tag{11}$$

Here $f_i\,(tra\bar{\tau}_i)$ is the stress function and ϵ_i represent the elongation behaviour of the fluid.

3. Formulation and Solution of the Problem

Consider immiscible and incompressible double layer flow of viscoelastic PTT fluid down on outside surface of a vertical cylinder of radius R under gravity. The density and viscosity of layer 1 and layer 2 is ρ_1, ρ_2 and η_1, η_2 respectively. The thickness of the layer1 and layer 2 is to be considered $h_1$and $h_2 - h_1$. Coordinate system is selected at the centre of the cylinder, in which z-axis is along the cylinder and r-axis along the radius of the cylinder. Assuming the flow is steady,laminar and neglecting the ambient air on the surface of the fluid.

The velocity field for both layers:

$$\bar{u}_i = u\big(0, 0, u_{iz}(r)\big)\text{and } \bar{\tau}_i = \bar{\tau}_i(r) \qquad i = 1, 2\,. \tag{12}$$

Boundary conditions are:

$$u_1 = 0 \qquad at \qquad r = R \tag{13}$$

$$u_1 = u_2 \qquad at \qquad r = R + h_1 \tag{14}$$

$$\tau_{1rz} = \tau_{2rz} \quad at \quad r = R + h_1 \tag{15}$$

$$\tau_{2rz} = 0 \qquad at \qquad r = R + h_2 \tag{16}$$

Using the assumptions and velocity field given in Eq. (12), the continuity Eq. (4) is identically satisfied and the corresponding non zero term of momentum equation from (5)-(7) and the constitution equation from (8)-(11) is reduce to

$$\frac{1}{r}\frac{\partial (r\tau_{irz})}{\partial r} = -\rho_i g_z \qquad i = 1, 2\,. \tag{17}$$

$$\eta_i\frac{\partial u_i}{\partial r} = \tau_{irz} + \frac{2\epsilon_i\lambda_i^2}{\eta_i^2}\tau_{irz}^3 \qquad i = 1, 2\,. \tag{18}$$

Integrating Eq. (17), and using boundary conditions given in Eq. (15) and (16) , we obtain

$$\tau_{1rz} = \frac{\rho_1 g}{2r}[(R + h_1)^2 - r^2] + \frac{\rho_2 g}{2r}[(R + h_2)^2 - (R + h_1)^2] \tag{19}$$

$$\tau_{2rz} = \frac{\rho_2 g}{2r}[(R + h_2)^2 - r^2] \tag{20}$$

The subscripts 1 and 2 represent layer 1 and layer 2 respectively.

Inserting, Eqs. (19) and (20) in Eq. (18), after integrating and making use of boundary conditions given in Eqs. (13) and (14) , we arrive at

$$u_1 = \frac{\rho_1 g}{2\eta_1}\left((R+h_1)^2(\log r - \log R) - \left(\frac{r^2}{2} - \frac{R^2}{2}\right)\right)$$
$$+\frac{\rho_2 g}{2\eta_1}\left((R+h_2)^2(\log r - \log R) - (R+h_1)^2(\log r - \log R)\right)$$
$$-\frac{2\epsilon_1}{\eta_1}\left(\frac{\lambda_1}{\eta_1}\right)^2\left(\frac{\rho_1 g}{2}\right)^3\left(\frac{(R+h_1)^6}{2}\left(\frac{1}{r^2}-\frac{1}{R^2}\right) - \left(\frac{r^4}{4}-\frac{R^4}{4}\right)\right.$$
$$\left.+3(R+h_1)^4(\log r - \log R) - 3(R+h_1)^2\left(\frac{r^2}{2}-\frac{R^2}{2}\right)\right)$$
$$-\frac{2\epsilon_1}{\eta_1}\left(\frac{\lambda_1}{\eta_1}\right)^2\left(\frac{\rho_2 g}{2}\right)^3\left(\frac{(R+h_2)^6}{2}\left(\frac{1}{r^2}-\frac{1}{R^2}\right) + \frac{(R+h_1)^6}{2}\left(\frac{1}{r^2}-\frac{1}{R^2}\right)\right.$$
$$\left.-3\frac{(R+h_2)^4(R+h_1)^2}{2}\left(\frac{1}{r^2}-\frac{1}{R^2}\right) + 3\frac{(R+h_2)^2(R+h_1)^4}{2}\left(\frac{1}{r^2}-\frac{1}{R^2}\right)\right)$$
$$-\frac{6\epsilon_1}{\eta_1}\left(\frac{\lambda_1}{\eta_1}\right)^2\left(\frac{\rho_1 g}{2}\right)^2\left(\frac{\rho_2 g}{2}\right)\left(\frac{(R+h_2)^2(R+h_1)^4}{2}\left(\frac{1}{r^2}-\frac{1}{R^2}\right) - \frac{(R+h_1)^6}{2}\left(\frac{1}{r^2}-\frac{1}{R^2}\right) - (R\right.$$
$$\left.+h_2)^2\left(\frac{r^2}{2}-\frac{R^2}{2}\right) + (R+h_1)^2\left(\frac{r^2}{2}-\frac{R^2}{2}\right)\right.$$
$$\left.+2(R+h_2)^2(R+h_1)^2(\log r - \log R) + (R+h_2)^4(\log r - \log R)\right)$$
$$\frac{6\epsilon_1}{\eta_1}\left(\frac{\lambda_1}{\eta_1}\right)^2\left(\frac{\rho_1 g}{2}\right)\left(\frac{\rho_2 g}{2}\right)^2\left(\frac{(R+h_2)^2(R+h_1)^4}{2}\left(\frac{1}{r^2}-\frac{1}{R^2}\right)\right.$$
$$+\frac{(R+h_1)^6}{2}\left(\frac{1}{r^2}-\frac{1}{R^2}\right) - (R+h_2)^2(R+h_1)^4\left(\frac{1}{r^2}-\frac{1}{R^2}\right)$$
$$+(R+h_2)^4(\log r - \log R) + (R+h_1)^4(\log r - \log R)$$
$$\left.-2(R+h_2)^2(R+h_1)^2(\log r - \log R)\right), \qquad (21)$$

$$u_2 = \frac{\rho_1 g}{2\eta_1}\left((R+h_2)^2(\log r - \log(R+h_2)) - \left(\frac{r^2}{2} - \frac{(R+h_1)^2}{2}\right)\right)$$
$$-\frac{2\epsilon_2}{\eta_2}\left(\frac{\lambda_2}{\eta_2}\right)^2\left(\frac{\rho_2 g}{2}\right)^3\left(\frac{(R+h_2)^6}{2}\left(\frac{1}{r^2}-\frac{1}{(R+h_1)^2}\right)\left(\frac{(R+h_1)^4}{4}-\frac{R^4}{4}\right)\right.$$
$$\left.+3(R+h_2)^4(\log r - \log(R+h_1)) - 3(R+h_1)^2\left(\frac{r^2}{2}-\frac{(R+h_1)^2}{2}\right)\right)$$
$$+\frac{\rho_1 g}{2\eta_1}\left((R+h_1)^2(\log(R+h_1) - \log R) - \left(\frac{(R+h_1)^2}{2}-\frac{R^2}{2}\right)\right)$$
$$+\frac{\rho_2 g}{2\eta_1}\left((R+h_2)^2(\log(R+h_1) - \log R) - (R+h_1)^2(\log(R+h_1) - \log R)\right)$$
$$-\frac{2\epsilon_1}{\eta_1}\left(\frac{\lambda_1}{\eta_1}\right)^2\left(\frac{\rho_1 g}{2}\right)^3\left(\frac{(R+h_1)^6}{2}\left(\frac{1}{(R+h_1)^2}-\frac{1}{R^2}\right) - \left(\frac{(R+h_1)^4}{4}-\frac{R^4}{4}\right)\right.$$
$$\left.+3(R+h_1)^4(\log(R+h_1) - \log R) - 3(R+h_1)^2\left(\frac{(R+h_1)^2}{2}-\frac{R^2}{2}\right)\right)$$
$$-\frac{2\epsilon_1}{\eta_1}\left(\frac{\lambda_1}{\eta_1}\right)^2\left(\frac{\rho_2 g}{2}\right)^3\left(\frac{(R+h_2)^6}{2}\left(\frac{1}{(R+h_1)^2}-\frac{1}{R^2}\right) + \frac{(R+h_1)^6}{2}\left(\frac{1}{(R+h_1)^2}-\frac{1}{R^2}\right)\right.$$
$$\left.-3\frac{(R+h_2)^4(R+h_1)^2}{2}\left(\frac{1}{(R+h_1)^2}-\frac{1}{R^2}\right) + 3\frac{(R+h_2)^2(R+h_1)^4}{2}\right.$$
$$\left.\left(\frac{1}{(R+h_1)^2}-\frac{1}{R^2}\right)\right) - \frac{6\epsilon_1}{\eta_1}\left(\frac{\lambda_1}{\eta_1}\right)^2\left(\frac{\rho_1 g}{2}\right)^2\left(\frac{\rho_2 g}{2}\right)\left(\frac{(R+h_2)^2(R+h_1)^4}{2}\left(\frac{1}{(R+h_1)^2}-\frac{1}{R^2}\right)\right.$$

$$-\frac{(R+h_1)^6}{2}\left(\frac{1}{(R+h_1)^2}-\frac{1}{R^2}\right)-(R+h_2)^2\left(\frac{(R+h_1)^2}{2}-\frac{R^2}{2}\right)+(R+h_1)^2\left(\frac{(R+h_1)^2}{2}-\frac{R^2}{2}\right)$$
$$+2(R+h_2)^2(R$$
$$+h_1)^2(\log(R+h_1)-\log R)+(R$$
$$+h_2)^4(\log(R+h_1)-\log R))\frac{6\epsilon_1}{\eta_1}\left(\frac{\lambda_1}{\eta_1}\right)^2\left(\frac{\rho_1 g}{2}\right)\left(\frac{\rho_2 g}{2}\right)^2\left(\frac{(R+h_2)^2(R+h_1)^4}{2}\left(\frac{1}{(R+h_1)^2}\right.\right.$$
$$\left.\left.-\frac{1}{R^2}\right)+\frac{(R+h_1)^6}{2}\left(\frac{1}{(R+h_1)^2}-\frac{1}{R^2}\right)-(R+h_2)^2(R+h_1)^4\left(\frac{1}{(R+h_1)^2}-\frac{1}{R^2}\right)+(R\right.$$
$$+h_2)^4(\log(R+h_1)-\log R)$$
$$\left.+(R+h_1)^4(\log(R+h_1)-\log R)-2(R+h_2)^2(R+h_1)^2(\log(R+h_1)-\log R)\right) \quad (22)$$

.

Volume flow rate for layer 1 and layer 2 is calculated as

$$Q_1=\int_R^{(R+h_1)}2\pi r\,u_1 dr \quad (23)$$

$$Q_2=\int_R^{(R+h_1)}2\pi r\,u_2\,dr \quad (24)$$

The analytical results for the flow rate are to large therefore, we present graphical results. On demand we can provide analytical results.

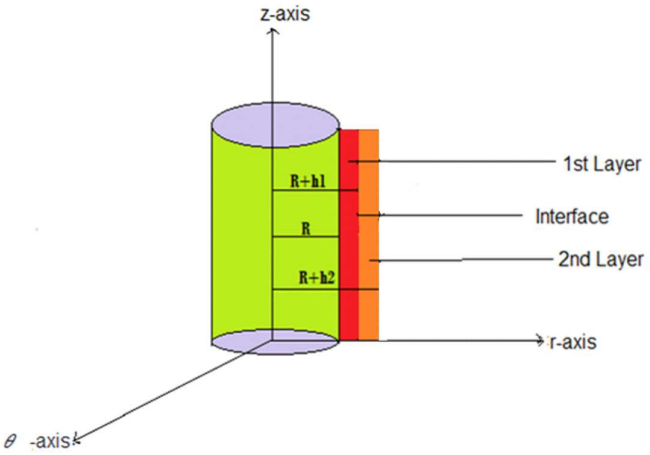

Figure 1: Geometry of a Viscoelastic Immiscible Double Layer Fluid Flow over outside Surface of a Vertical Cylinder

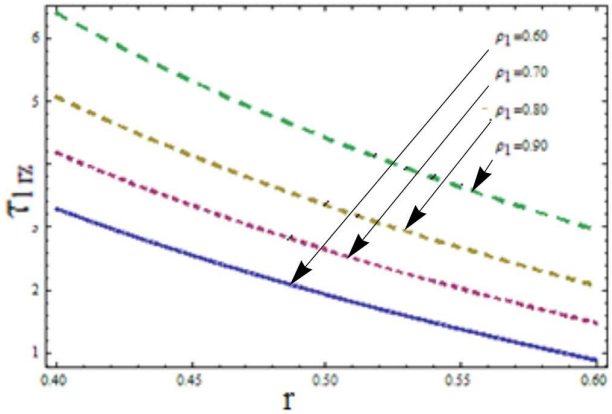

Figure 2: Profile of shear stress of layer 1 for different values of ρ_1 at fixed values of $R = 0.4$, $h_1 = 0.2$, $h_2 = 0.45$, $\rho_2 = 0.40$ and $g = 9.8$.

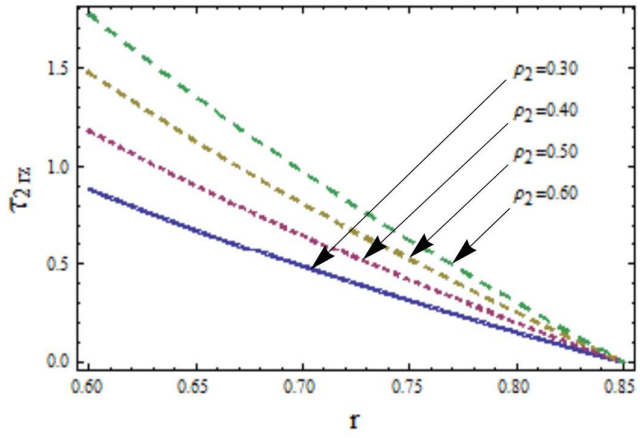

Figure 3:Profile of shear stress of layer 2 for different values of ρ_2 at fixed values of $R = 0.4$, h_2= 0.45 and g = 9.8.

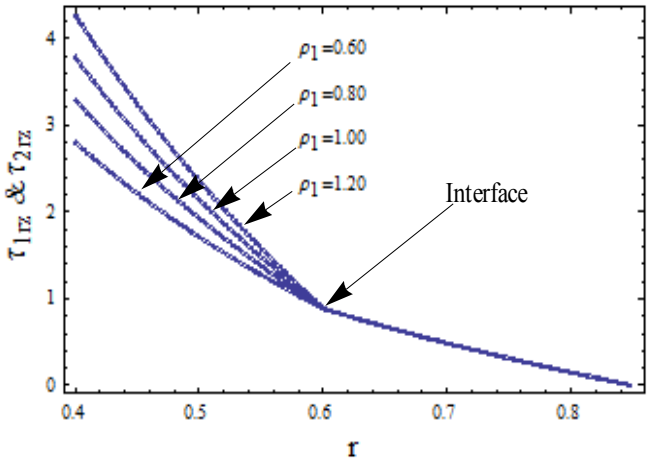

Figure 4: Profile of shear stress of layer 1 and layer 2 for different values ofρ_1 at fixed values of $R = 0.4$, $h_1 = 0.2$, $h_2 = 0.45$,$\rho_2 = 0.30$ and g =9.8.

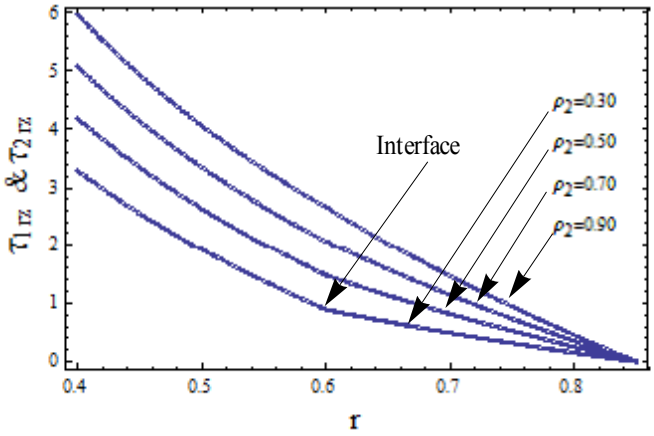

Figure 5: Shear stress of layer 1 and layer 2 for different values of$\rho_2$at fixed values of $R = 0.4$, $h_1 = 0.2$, $h_2 = 0.45$, $\rho_1 = 0.80$ and g =9.8.

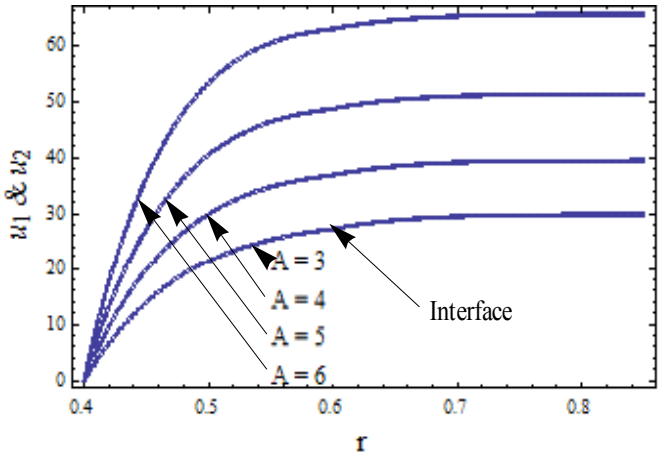

Figure 6: Velocity profile of layer 1 and layer 2 for different value of A at fixed values of $L = 3$,$P = 6.5$ and $K = 5$.

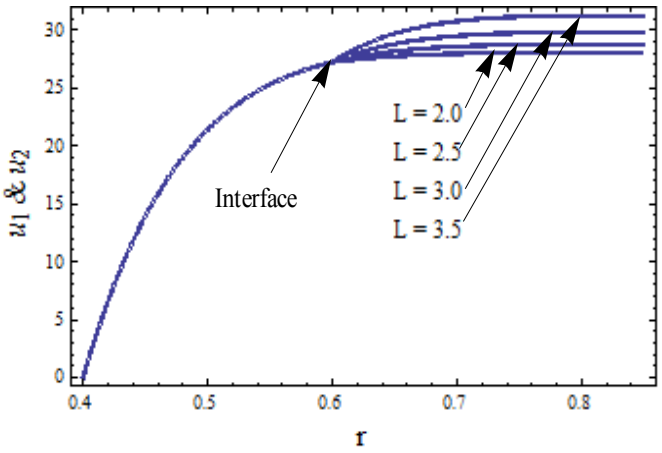

Figure 7: Velocity profile of layer 1 and layer 2 for different valuesof L at fixed values of $A = 3$, $P = 6.5$ and $K = 5$.

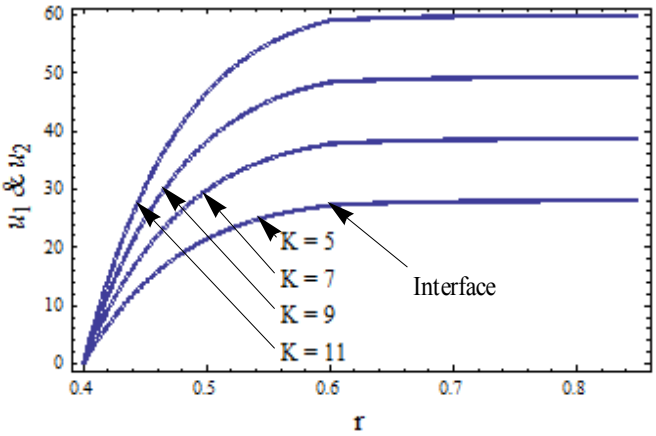

Figure 8: Velocity profile of layer 1 and layer 2 for different values of K at fixed values of $A = 3$, $L = 2$ and $P = 6.5$.

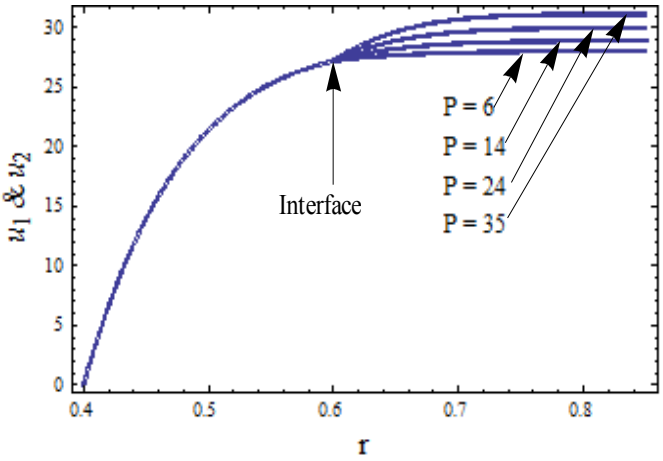

Figure 9: Velocity profile of layer1 and layer 2 for different values of P at fixed values of $A = 3$, $L = 2$ and $K = 5$.

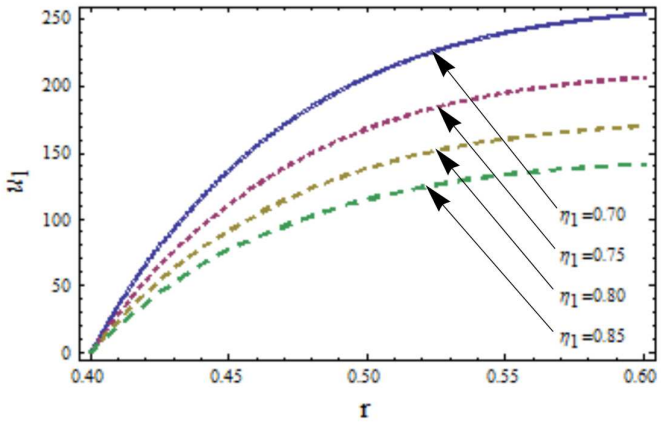

Figure 10: Velocity profile of layer 1 for different values of $\eta_1$at fixed values of $\epsilon_1 = 2.2$,$\lambda_1 = 2.0$, $\rho_1 = 0.80$, $\epsilon_2 = 2.0$, $\lambda_2 = 1.50$, $\rho_2 = 0.50$, $\eta_2 = 0.60$ and $g = 9.8$.

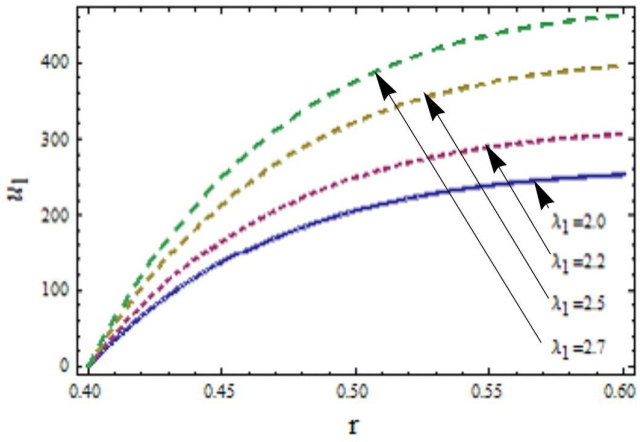

Figure 11: Velocity profile of layer 1 for different values of λ_1 at fixed values of $\epsilon_1 = 2.2$, $\eta_1 = 2.0$, $\rho_1 = 0.80$, $\epsilon_2 = 2.0$, $\lambda_2 = 1.50$, $\rho_2 = 0.50$, $\eta_2 = 0.60$ and $g = 9.8$.

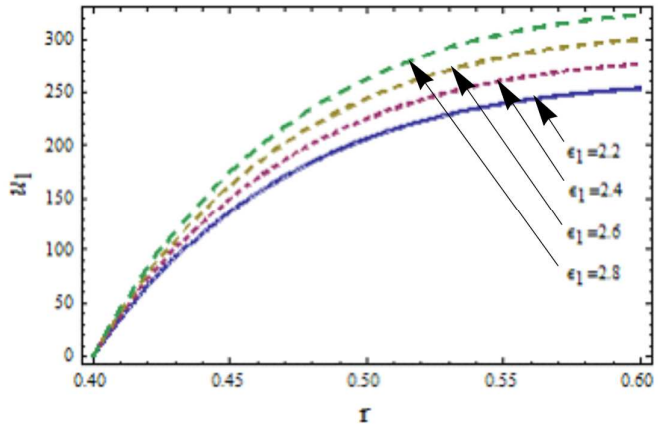

Figure 12: Velocity profile of layer 1 for different values of ϵ_1 at fixed values of $\lambda_1 = 2.0, \eta_1 = .70, \rho_1 = 0.80, \epsilon_2 = 2.0, \lambda_2 = 1.50, \rho_2 = 0.50, \eta_2 = 0.60$ and $g = 9.8$.

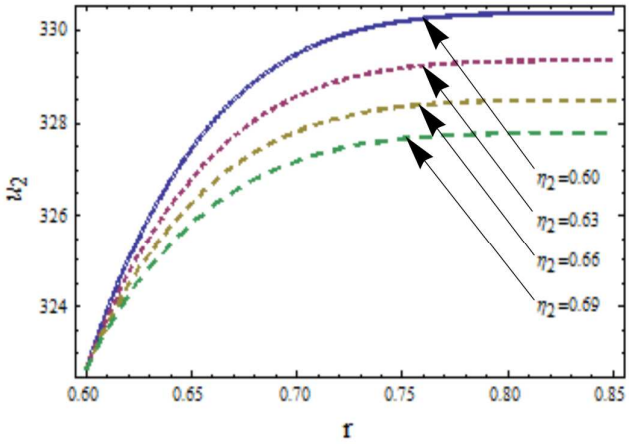

Figure 13: Velocity profile of layer 2 for different values of η_2 at fixed values of $\epsilon_1 = 2.8, \lambda_1 = 2.0, \eta_1 = 0.70, \rho_1 = 0.80, \epsilon_2 = 2.0, \lambda_2 = 1.50, \rho_2 = 0.50$ and $g = 9.8$.

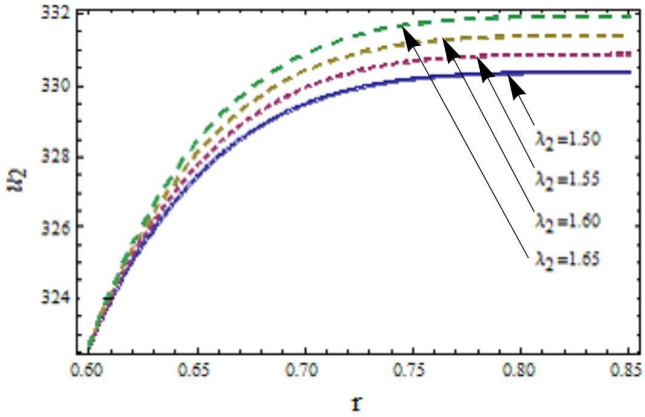

Figure 14: Velocity profile of layer 2 for different values of $\lambda_2$at fixed values of $\epsilon_1 = 2.8, \lambda_1 = 2.0, \eta_1 = .70, \rho_1 = 0.80, \epsilon_2 = 2.0, \eta_2 = 0.60, \rho_2 = 0.50$ and $g = 9.8$.

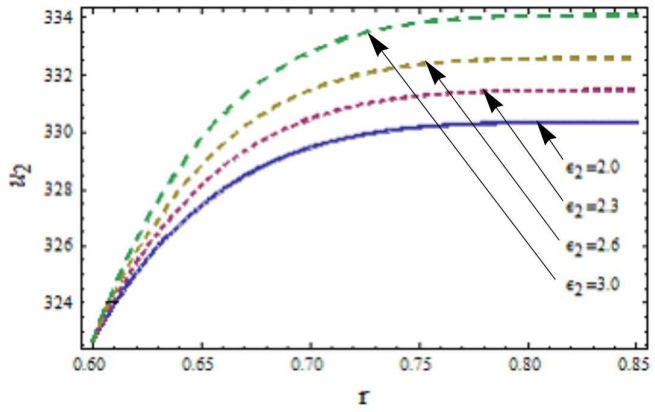

Figure 15: Velocity profile of layer 2 for different values of $\epsilon_2$at fixed values of $\epsilon_1 = 2.8, \lambda_1 = 2.0, \eta_1 = 0.70, \rho_1 = 0.80, \lambda_2 = 1.50, \eta_2 = 0.60, \rho_2 = 0.50$ and $g = 9.8$.

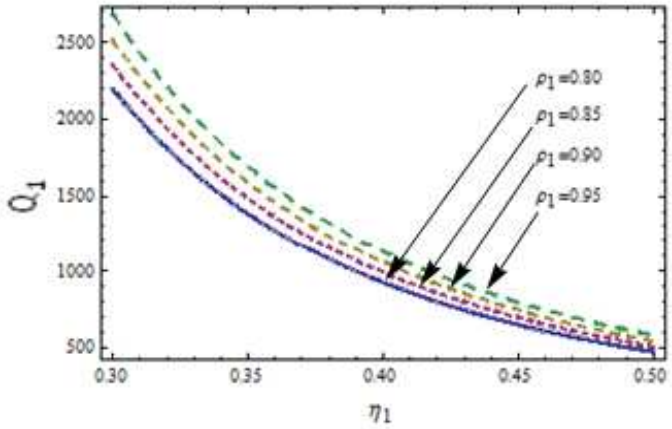

Figure 16: Flow rate profile of layer 1 for different values of $\rho_1$at fixed values of $\epsilon_1 = 2.3, \lambda_1 = 2.0, \epsilon_2 = 2, \eta_2 = 0.7, \lambda_2 = 1.5, \rho_2 = 0.60$ and $g = 9.8$.

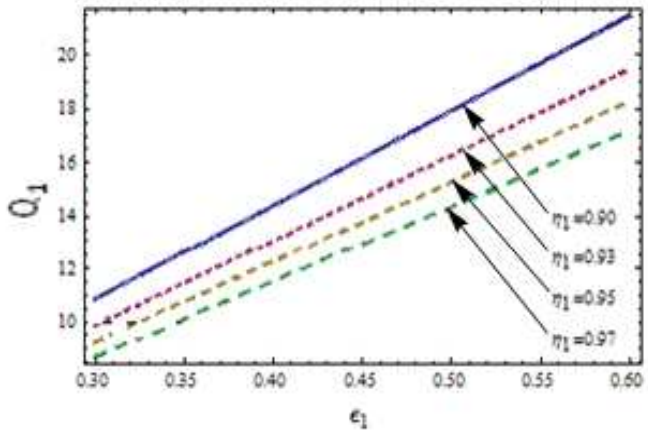

Figure 17: Flow rate profile of layer 1 for different values of $\eta_1$at fixed values of $\rho_1 = 0.8, \lambda_1 = 2.0, \epsilon_2 = 2, \eta_2 = 0.7, \lambda_2 = 1.5, \rho_2 = 0.60$ and $g = 9.8$.

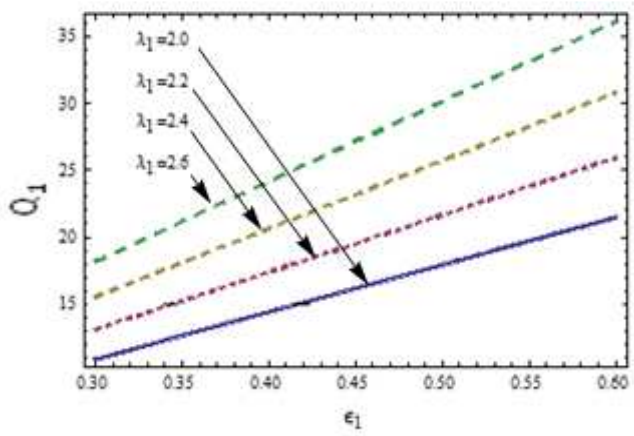

Figure 18: Flow rate profile of layer 1 for different values of $\lambda_1$at fixed values of $\rho_1 = 0.8, \eta_1 = 0.90,\ \epsilon_2 = 2,$ $\eta_2 = 0.7, \lambda_2 = 1.5, \rho_2 = 0.60$ and $g = 9.8$.

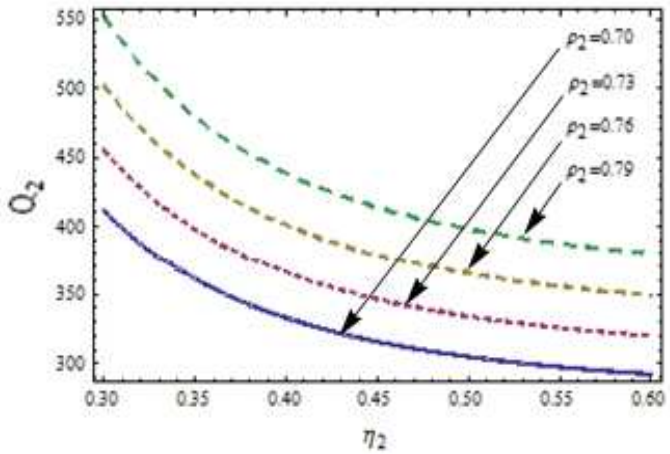

Figure 19: Flow rate profile of layer 2 for different values of $\rho_2$at fixed values of $\epsilon_1 = 2.3,\ \lambda_1 = 2.0,\ \rho_1 = 0.80, \eta_1 = 0.90,\ \epsilon_2 = 2,\ \lambda_2 = 1.5,$ and $g = 9.8$.

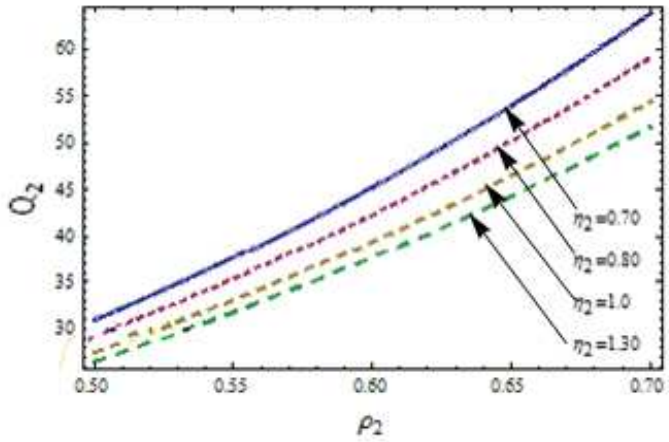

Figure 20: Flow rate profile of layer 2 for different values of $\eta_2$at fixed values of $\epsilon_1 = 2.3,\ \lambda_1 = 2.0,\ \rho_1 = 0.80, \eta_1 = 0.90,\ \epsilon_2 = 2,\ \lambda_2 = 1.5,$ and $g = 9.8$.

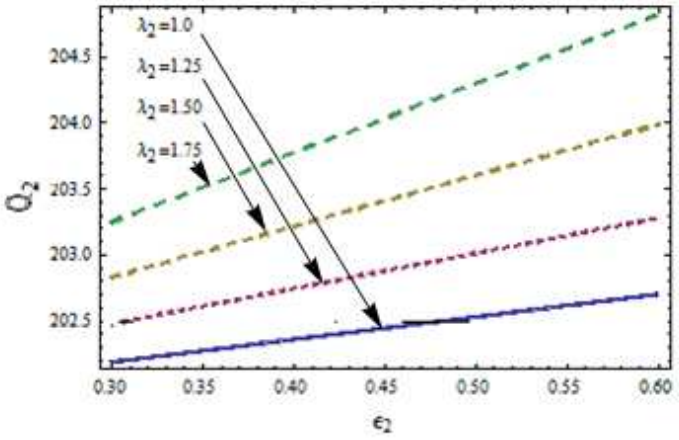

Figure 21: Flow rate profile of layer 2 for different values of $\lambda_2$at fixed values of $\epsilon_1 = 2.3,\ \lambda_1 = 2.0,\ \rho_1 = 0.80, \eta_1 = 0.90,\ \eta_2 = 0.70,\ \rho_2 = 0.60$ and $g = 9.8$.

4. RESULTS AND DISCUSSION

Analysis of the gravity driven motion of a superposition of two immiscible visco-elastic PTT fluids flowing down an outer surface of a vertical cylinder is studied. The constitutive equations are solved exactly with the help of no slip condition at the cylinder wall, free surface condition without surface tension and the interface condition. For better understanding Figs. 2-21 are plotted. Figures 2 and 3 represent the effect of fluid density ρ_1 and ρ_2 on the gradual development of the shear stress with respect to time r for fixed values of other physical quantities, respectively. It is clear from both the figure that increasing density ρ_1 and ρ_2 shear stresses also increases. One can observe the gradual variation of the shear stress in both the layers when the fluid viscosities are changed. The combine graph of shear stress is shown in Figs. 4 and 5, where interface is selected here at $r = 0.6$.

Figures 6-9 show a plot of the velocity field for layer 1 and 2 given by Eqs. (21) and (22) generated for different values of A, L, K and P for the following system of parameters (i) $L = 3,\ P = 6.5, K = 5$ (ii)$A = 3,\ P = 6.5, K = 5$ (iii)$A = 3,\ L = 2, K = 5$ (iv) $A = 3,\ L = 2, K = 5$ respectively, where $A = \rho_1 g/2, L = \rho_2 g/2, K = 2\,\epsilon_1\lambda_1^2/\eta_1^2$ and $P = 2\,\epsilon_2\lambda_2^2/\eta_2^2$. It is clear from these figures that the velocity profile increases while increasing the parameter A and L. Velocity of the layer near the wall increases rapidly in parabolic form, while, the velocity of second layer increases slowly and this increase is seems to be almost linear. For large values of L the speed of layer 2 is seems to be more clear and rapid. The effects of viscosities η_1, η_2, relaxation parameters$\lambda_1, \lambda_2$and elongation parameters ϵ_1, ϵ_2 on both the layers are plotted in Figs. 10-15. Here it is noticed that increasing viscosity η_1 of layer 1 and η_2 of layer 2, the velocity of both the layers decreases as shown in Figs. 10 and 11, while, increasing relaxation parameter λ_1, λ_2 and elongation parameters ϵ_1, ϵ_2 the velocities of both the layers increases. Figures 16-21 are plotted for variation of flow rate for layer 1 and layer 2. In which Figs. 16-18 are plotted for flow rate of layer 1 versus elongation parameter for different values of density ρ_1 , viscosity η_1, and relaxation parameter λ_1 , respectively. Here, it is noticed that flow rate increases as the density η_1 and the relaxation parameter $\lambda_1$of layer 1 increases, while it decreases as the viscosity η_1 increases. Figures 19-21 are plotted for variation of flow rate of layer 2, versus η_2, $\rho_2$and ϵ_2, for different values of ρ_2, η_2 and λ_2, respectively. It can be seen that increasing ρ_2 and λ_2 flow rate increases, while increasing η_2 flow rate decreases.

5. Conclusions

The constitutive equations governing the flow of double layer PTT fluid over outside surface of a vertical cylinder are solved exactly for velocity field, flow rate and shear stresses in case of inner and outer layer. The following conclusions are made during this analysis:

i. Velocity of both the layers decreases as the viscosity of fluid layers increases, while shear stress increases in both layers.
ii. As expected, the velocities and flow rate of layer 1 and layer 2 increasesas the relaxation and elongation parameters increases.
iii. The gradual variations of the shear stress in layer 1 and layer 2 are observed as the fluid densities are varied. The turning point of the fluid shear stress is also observed here at the interface.

iv. The velocity of outer layer is greater than the inner layer due to no slip condition with the cylinder wall for all involved physical parameters.

v. Flow rate of both the layers increases while increasing the relaxation parameter, elongation parameter and density of fluids. On the other hand, it decreases as the fluid become more viscous.

REFERENCES

1. T. Gul, S. Islam, K. khan, M. A. Khan, R. A. Shah, A. Gul, M. Ullah, 2014. Thin Film Flow Analysis of a MHD Third Grade Fluid on a Vertical Belt With no -slip Boundary Conditions. J. App. Envir. Sci., 4 (10): 71-84.
2. T. Gul, Mubashir, M. A. Khan, S. Islam, R. A. Shah, I. Khan, M. Idrees, S. Shafie, 2015. Influence of Slip Condition on MHD Thin Film Flow of a Third Grade Fluid over a Vertical Belt with Temperature Dependent Viscosity. J. App. Envir. Sci., 5 (3): 22-30.
3. T. Hayat and M. Sajid, 2007. On analytic solution of thin film flow of a fourth grade fluid down a vertical cylinder. Phy. Lett. A, 361(4): 316-322.
4. M. Sajid, A. M. Siddiqui and T. Hayat, 2007. Wire coating analysis using MHD Oldroyd 8- constant fluid. Int. J. Eng. Sc, 45: 381-392.
5. T. G. Smith and J. O. Wilkes, 1975. Laminar Free-Surface Flow into a Vertical Cylinder. Computers and Fluids, 3: 51-68.
6. R. B. Bird, W. E. Stewart and E. N. Lightfoot, Transport phenomena, 1960. Transport phenomena. John Willy and Sons, New York. 7.
7. J. N. Kapur and J. B. Shukla, 1964. On the unsteady flow of two incompressible immiscible fluids between two plates. Journal of applied Mathematics and Mechanics, 44(6): 268-269.
8. J. N. Kapur and J. B. Shukla, 1964. The flow of incompressible immiscible fluids between two plates. Appl. Sci. Res, 13(1): 55-60.
9. Sacheti, N.C.(1974). Plane coquette flow of two immiscible incompressible non-Newtonian fluids with uniform suction at the stationary plate. March: 527-540.
10. A. Juel, J. M. Burgess, W. D. McCormick, J. B. Swift and H. L. Swinney, 2000. Surface tension-driven convection Patterns in two liquid layers, Physica D, 143: 169–186.
11. H. M. Chu, W. L. Li and Y. P. Chang, 2006. Thin film elastohydrodynamic lubrication a power-law fluid model. Tribology International, 39: 1474–1481.
12. K. Kim and H. S. Kwak, 2012. Analytical study of non-Newtonian double layer coating liquid flows in optical fiber manufacturing, Applied Mechanics and Materials 224: 260-263.
13. B. S. Dandapat and S. K. Singh, 2012. Two-layer film flow over a rotating disk, Common Nonlinear Sci. Numer. Simulat. 17: 2854–2863.
14. Zeeshan, R. A. Shah, S. Islam and A. M. Siddique, 2013. Double-layer Optical Fiber Coating Using Viscoelastic Phain-Thein Tanner Fluid. New York Science Journal, 10: 66-73.